....

Characterization of a common precursor population for dendritic cells

Gloria Martínez del Hoyo, Pilar Martín, Héctor Hernández Vargas, Sara Ruiz, Cristina Fernández Arias & Carlos Ardavín

Department of Cell Biology, Faculty of Biology, Complutense University, 28040 Madrid, Spain

....

Dendritic cells (DCs) are essential for the establishment of immune responses against pathogens and tumour cells, and thus have great potential as tools for vaccination and cancer immunotherapy trials. Experimental evidence has led to a dual DC differentiation model, which involves the existence of both myeloid- and lymphoid-derived DCs[1]. But this concept has been challenged by recent reports demonstrating that both CD8^{−} and CD8^{+} DCs, considered in mice as archetypes of myeloid and lymphoid DCs respectively, can be generated from either lymphoid[2–4] or myeloid progenitors[3,4]. The issue of DC physiological derivation therefore remains an open question. Here we report the characterization of a DC-committed precursor population, which has the capacity to generate all the DC subpopulations present in mouse lymphoid organs—including CD8^{−} and CD8^{+} DCs, as well as the B220^{+} DC subset—but which is devoid of myeloid or lymphoid differentiation potential. These data support an alternative model of DC development, in which there is an independent, common DC differentiation pathway.

Current controversy about the physiological derivation of DCs results largely from the lack of information about DC progenitors. To obtain insights into the developmental origin of DCs, we searched for a murine DC precursor in the blood cell fraction expressing the DC-specific integrin CD11c. Blood CD11c^{+} cells can be subdivided into MHC class II (MHC-II)[+] and MHC-II^{−} subsets (Fig. 1A, a). Phenotypic analyses (not shown) revealed that CD11c^{+} MHC-II^{+} cells corresponded to CD4^{−} CD8^{−} HSA^{+} F4/80^{+} CD62L^{−} blood DCs, similar to splenic CD8^{−} DCs (ref. 5), and allowed us to design the method used here to purify the MHC-II^{−} subset (Fig. 1A, a–c). CD11c^{+} MHC-II^{−} cells displayed ultrastructural characteristics of undifferentiated cells (Fig. 1B), and were B220^{+}, CD19^{−}, CD43^{+}, CD11b^{+} and 50% were Thy-1^{+} (Fig. 1A, b). They expressed FcRγ, CD44 and the homing receptor CD62L, and were negative for the cytokine receptors c-kit, IL-7Rα and IL-3Rα, the B-cell/DC-related molecules CD40, CD86 and DEC-205, the macrophage marker F4/80 and the granulocyte antigen Gr-1. The phenotype of CD11c^{+} MHC-II^{−} cells, representing around 5% (5.4 ± 0.8, n = 4) of blood mononuclear cells, corresponded to that of a progenitor population, as they were negative for lineage markers and expressed early precursor markers, though this phenotypic profile does not allow us to correlate them to lymphoid or myeloid precursors. Importantly, CD11c^{+} MHC-II^{−} cells neither corresponded with monocytes nor included monocytes, because the last express F4/80 and Gr-1, but are negative for CD11c and CD43. (Comparative phenotype profile of DC-precursors versus monocytes: DC-precursors are CD11c^{+} B220^{+} CD43^{+} HSA^{−} Gr-1^{−} F4/80^{−} whereas monocytes are CD11c^{−} B220^{−} CD43^{−} HSA^{+} Gr-1^{+} F4/80^{+}; C.A., unpublished data). Moreover, DCs were not generated from monocytes after intravenous transfer into irradiated mice (C.A, unpublished data).

We then determined the reconstitution potential of CD11c^{+} MHC-II^{−} cells transferred into γ-irradiated recipients using an Ly5.1/5.2 system to trace donor-type Ly5.2^{+} cells. B220-depleted splenic DC-enriched fractions were analysed for donor-type DCs. Both Ly5.2^{+} CD8^{−} and CD8^{+} DCs were detected after 7 days

(Fig. 2a); by day 14 the number of donor-type DCs was similar to that of DCs in control spleens[5], indicating that CD11c^{+} MHC-II^{−} cells had the potential to fully reconstitute the CD8^{−} and CD8^{+} DC populations. Donor-type DCs displayed similar phenotypic characteristics to control splenic DCs, and their CD8^{−}:CD8^{+} ratio was 65:35, 50:50 and 35:65 at days 7, 10 and 14 respectively. Because the CD8^{−}:CD8^{+} ratio of splenic DCs reconstituted from bone marrow precursors was 70:30 after 3 weeks, as in the spleen of control mice[2], and as CD8^{+} DCs have been claimed to derive from the CD8^{−} DC subset[6], our data on DC derivation from CD11c^{+} MHC-II^{−} precursors suggest the extinction of the CD11c^{+} MHC-II^{−} precursors during the third week after transfer. This is in agreement with the low DC reconstitution observed 21 days after transfer (not shown). The extinction time of CD11c^{+} MHC-II^{−} precursors after transfer and their DC reconstitution capacity is in agreement with those described for bone marrow myeloid and lymphoid progenitors (3–4 weeks; refs 3 and 4) and for thymic CD4^{low} lymphoid precursors (3 weeks; ref. 7). Analysis of the absolute number of Ly5.2^{+} DCs generated from CD11c^{+} MHC-II^{−} precursors (Fig. 2b) suggests that DC differentiation from this population involves a rapid cell expansion concomitant with the overall splenic reconstitution. (Total spleen cells obtained after reconstitution of irradiated mice with 4×10^4 bone marrow cells were as follows: 7 days, 15×10^6; 10 days, 50×10^6; 14 days, 130×10^6 cells. Data are from an experiment representative of four with similar results.)

Analysis of the migration to the spleen of the CD11c^{+} MHC-II^{−} precursors, performed after transfer of CFSE-labelled precursors revealed that around 1% of the injected CD11c^{+} MHC-II^{−} precursors (that is, 5×10^3 cells) were detected in the spleen along the first week (not shown; CFSE, carboxyfluorescein diacetate succinimidyl ester). Therefore, as the total Ly5.2^{+} DCs generated were approximately 30×10^3 by day 7 (Fig. 2b), these data indicate that the number of CD11c^{+} MHC-II^{−} precursors had increased by a factor of six during the first week. In order to give added support to these data on the expansion of CD11c^{+} MHC-II^{−} precursors, their *in vivo* proliferation rate was assessed after CFSE-labelling of purified Ly5.2^{+} CD11c^{+} MHC-II^{−} precursors and transfer into irradiated mice. As illustrated in Fig. 2c, the CFSE profile of CD11c^{+} cells at day 7 after precursor transfer, after gating for Ly5.2^{+} cells, showed that CD11c^{+} MHC-II^{−} precursors underwent up to 3 cell divisions after the first week, in accordance with the sixfold expansion in numbers observed by day 7. These data reflect the strong expansion of CD11c^{+} MHC-II^{−} precursors occurring during DC reconstitution, and are in agreement with those reported for DC generation from lymphoid and myeloid progenitors[4].

We have recently found a CD11c^{+} MHC-II^{−} B220^{+} CD40^{−} DC subpopulation, which we will refer to here as B220^{+}-DCs, characterized by its low stimulatory potential and capacity to produce interferon (IFN)-α after viral stimulation[8]. Therefore we analysed non-B220-depleted splenic DC-enriched fractions for the presence of donor-type B220^{+}-DCs. Figure 2d shows the analysis of DC reconstitution 10 days after transfer of CD11c^{+} MHC-II^{−} precursors, performed in parallel on B220^{+} or B220^{−} splenic DC-enriched fractions. Both donor-type CD11c^{+} B220^{+} DCs and CD11c^{+} B220^{−} DCs (the latter corresponding to CD8^{−} plus CD8^{+} DCs) were produced. The kinetics of B220^{+}-DC production from DC-precursors paralleled that of B220^{−} DCs; that is, donor-type B220^{+}-DCs were detected at day 7 and peaked by day 14 (Fig. 2b). The donor-type B220[+]:B220[−] DC ratio and cell number at day 7, 10 and 14 was similar to that obtained from bone marrow precursors (not shown), demonstrating that differentiation from CD11c^{+} MHC-II^{−} precursors included the full reconstitution of B220^{+}-DCs. In order to determine the capacity of B220^{+}-DCs generated from CD11c^{+} MHC-II^{−} precursors to produce IFN-α, as described for B220^{+}-DCs from control mice[8], FACS-sorted Ly5.2^{+} B220^{+}-DCs were analysed for IFN-α production (FACS, fluorescence-activated cell

sorting). Incubation with Sendai virus induced IFN-α mRNA expression by donor-type B220[+]-DCs, as assessed by RT–PCR (PCR after reverse transcription of RNA) analysis (Fig. 2e).

Analysis of the thymus, spleen, bone marrow and blood revealed that no T cells, B cells, monocytes, macrophages or granulocytes were generated from CD11c^{+} MHC-II^{−} precursors (Fig. 3A). Furthermore, neither B cell, nor myeloid cell, nor NK cell formation was observed after culture of CD11c^{+} MHC-II^{−} precursors under specific conditions for the differentiation of these cell lineages (not shown; see Methods for details). The percentage of DC reconstitution from CD11c^{+} MHC-II^{−} precursors was significantly lower for thymic DCs than for splenic DCs (0.1% versus 7% at day 7; not shown), suggesting a reduced thymus homing capacity of CD11c^{+} MHC-II^{−} precursors. In summary, blood CD11c^{+} MHC-II^{−} cells represent a DC-committed precursor population, hereafter named DC-precursors, with capacity to fully reconstitute all splenic DC subpopulations, including CD8^{−} DCs, CD8^{+} DCs and B220^{+}-DCs, but devoid of lymphoid/myeloid differentiation potential.

Although it has been shown that DCs can be reconstituted from either lymphoid or myeloid precursors[2,3], the DC differentiation pathway under physiological conditions, and consequently the functional relevance of DC-precursors in this process, remain to be clarified. In an attempt to trace the lineage derivation of DC-precursors, we analysed their expression of the transcription factors Pax-5 and SCL which are expressed by lymphoid and myeloid precursors in a mutually exclusive way[9,10]. RT–PCR analysis of FACS-sorted DC-precursors revealed that they expressed neither Pax-5 nor SCL-mRNA (Fig. 3B). In addition, flow cytometry analysis of the expression of the cytokine receptor IL-7Rα, defining lymphoid-lineage commitment[11], revealed that DC-precursors were IL-7Rα[−] (Fig. 1A, b). These data might indicate that DC-precursors are located in a downstream position in the lymphoid and/or myeloid differentiation pathway involving Pax-5, IL-7Rα and SCL downregulation; this would be in agreement with the non-expression by DC-precursors of the c-kit receptor (Fig. 1A, b) defining early haematopoietic precursors[12]. Alternatively, a multipotential
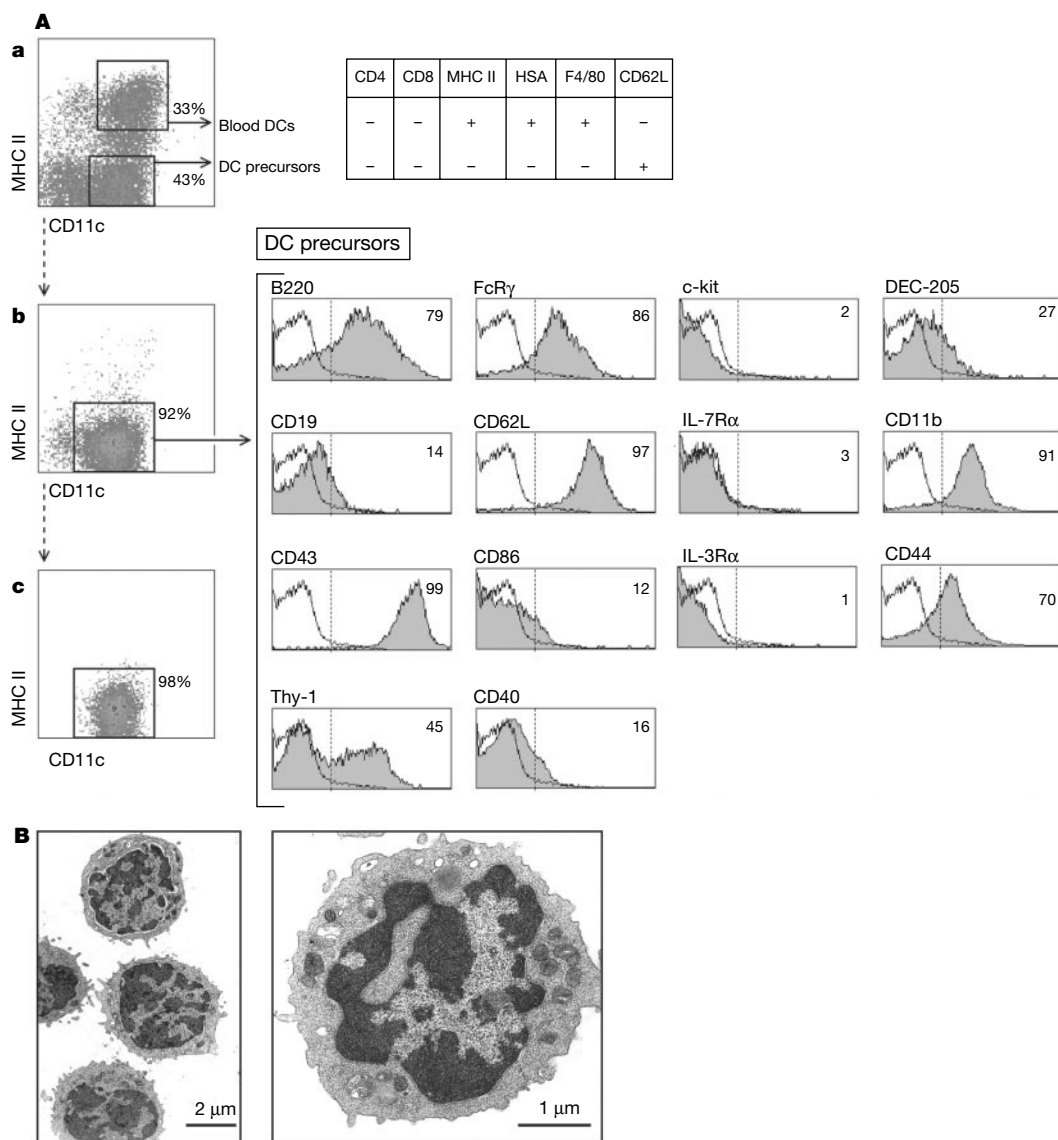

Figure 1 Identification of DC-precursors in mouse peripheral blood. **A**, **a**, Definition of CD11c^{+} MHC-II^{+} and CD11c^{+} MHC-II^{−} blood cells performed on blood DC-enriched fractions. **b**, Phenotype of DC-precursors after isolation by a magnetic bead depletion method yielding a purity >90%. The percentage of cells with a fluorescence intensity over the dotted vertical lines, corresponding to the background staining shown in the B220 histogram (white profile), is indicated. **c**, Purification of DC precursors by magnetic cell sorting (MACS), after magnetic bead depletion (purity >95%). **B**, Electron micrographs of FACS-sorted DC precursors (DC-precursor size: $4.5 \pm 0.2\,\mu m$, $n = 4$).

1044 NATURE | VOL 415 | 28 FEBRUARY 2002 | www.nature.com

lymphoid/myeloid progenitor[13,14] may generate DC-precursors independently from lymphoid and myeloid progenitors. Whether physiologically DCs are generated as the result of a dual contribution of lymphoid and myeloid progenitors as proposed[3,4], and/or independently from DC-precursors, has to be unravelled. (A model of DC development relying on a common DC differentiation pathway from DC-precursors is presented as Supplementary Information).

To explore whether DC-precursors were endowed with type-I IFN producing capacity upon viral stimulation, characterizing human plasmacytoid cells[15,16], purified DC-precursors were analysed for the production of IFNα after incubation with Sendai virus. As assessed by RT–PCR analysis, no IFNα–mRNA was detected in DC-precursors after viral stimulation (Fig. 3B). Consequently, DC-precursors are not functionally equivalent to plasmacytoid cells, whose mouse counterpart has not been characterized yet, though their role could be fulfilled at least partly by B220[+] -DCs, endowed with IFN-α production capacity, and displaying specific phenotypic characteristics[8]. (Comparative phenotype profiles of DC-precursors versus B220^{+} DCs were as follows. DC-precursors are MHC-II^{–} CD4^{–} CD8^{–} HSA^{–} CD62L^{+} CD11b^{+} whereas B220^{+} DCs are MHC-II^{+} CD4^{+} CD8^{+} HSA^{+} CD62L^{–} CD11b^{–} (ref. 8).

Finally, we investigated whether DC-precursors were involved in viral infection-induced inflammatory responses involving intensive DC recruitment. We analysed the DC-precursor population in the popliteal lymph nodes after injection of mouse mammary tumour virus (MMTV). MMTV induced a massive increase in lymph node DCs (Fig. 3C, a) that peaked by day 6 and declined afterwards, as described for the overall response to MMTV[17]. Two days after MMTV injection, CD11c^{int} MHC-II^{–} cells with an identical phenotype to blood DC-precursors were identified (Fig. 3C, b). These cells were found from day 2 to day 5 after injection, being undetectable after day 6 (not shown). These results suggest that MMTV-induced increase in DCs occurred by recruitment of blood DC-precursors and subsequent intranodal DC differentiation. In support of this concept, no significant increase in lymph node DCs (by day 3; Fig. 3C, a) or in CD11c^{int} MHC-II^{–} cells (by day 2; Fig. 3C, b) was induced by MMTV after anti-CD62L treatment, indicating that anti-CD62L blocked DC-precursor homing. It is important to note that anti-CD62L could not have blocked mature DC homing to the lymph node because blood DCs were CD62L-negative (Fig. 1A, a). Regarding DC-precursor expansion during DC differentiation accompanying MMTV infection, around 7×10^3 (7,300 ± 1,600, $n = 3$) DC-precursor-like CD11c^{int} MHC-II^{–} cells were detected at
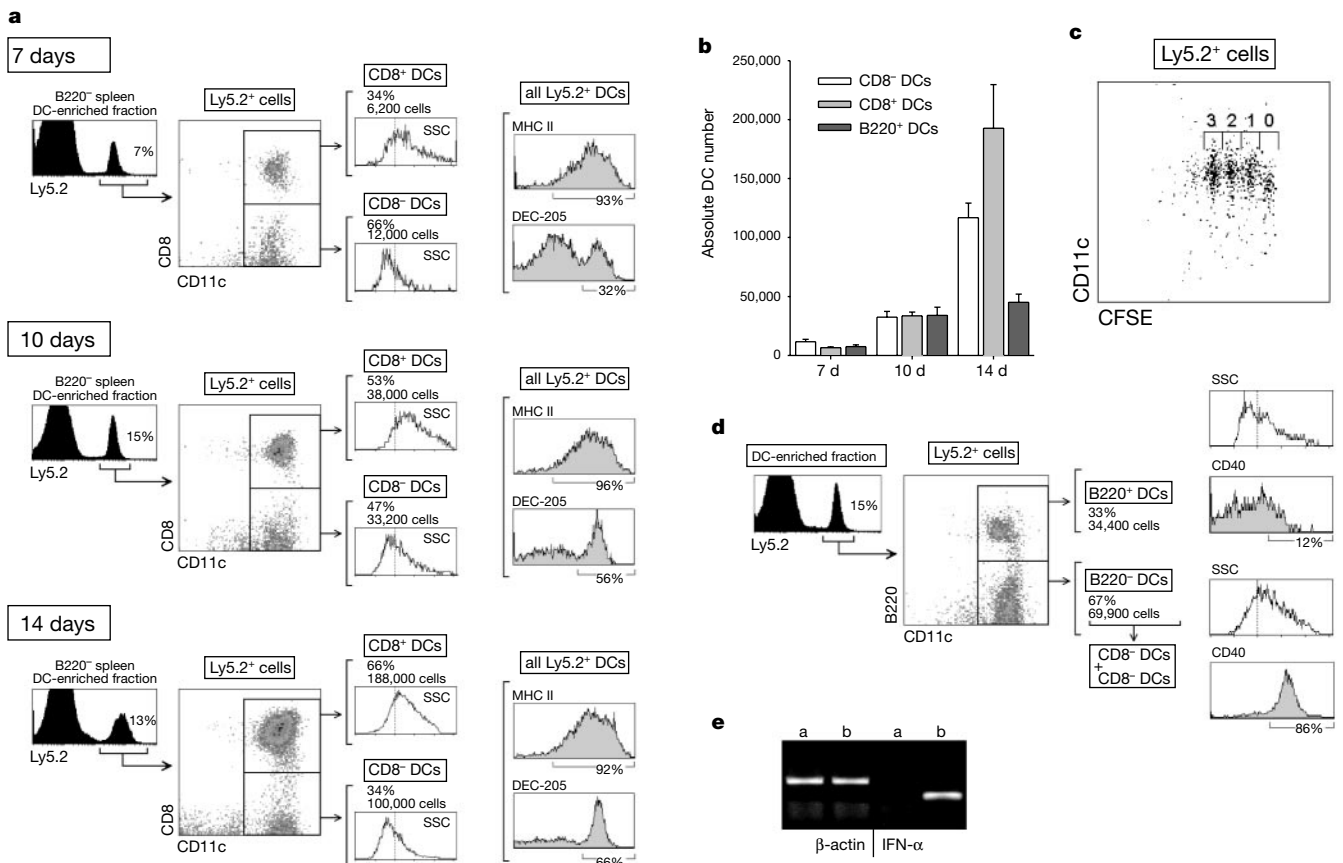
Figure 2 DC reconstitution by blood DC-precursors. **a**, CD8^{–} and CD8^{+} DC reconstitution from DC-precursors. Contour plots correspond to the CD11c versus CD8 expression of Ly5.2^{+} cells analysed on B220^{–} DC-enriched splenic fractions. The percentage and absolute number of CD8^{–} and CD8^{+} DCs is indicated over the side scatter histograms. Grey histograms show MHC-II and DEC-205 expression by donor-type splenic DCs. These results are representative of four independent experiments with similar results. **b**, Splenic CD8^{–}, CD8^{+} and B220^{+}-DC reconstitution potential of DC-precursors. Histograms show the absolute number of reconstituted Ly5.2^{+} CD8^{–}, CD8^{+} or B220^{+}-DCs at day 7, 10 and 14 after DC-precursor transfer. Data represent the mean ± s.d. ($n = 4$). **c**, In vivo expansion of DC-precursors during DC reconstitution. Contour plots show CFSE-labelling versus CD11c expression after gating for Ly5.2^{+} cells on splenic DC-enriched fractions, analysed at day 7 after DC-precursor transfer. The number of cell divisions undergone by DC-precursors is indicated. **d**, B220[+]-DC generation by DC-precursors analysed on DC-enriched splenic fractions avoiding depletion with anti-B220, 10 days after DC-precursor transfer. The percentage and absolute number, as well as the side scatter and CD40 expression (grey profiles) of donor-type B220^{+}, and B220^{–}DCs (which include prototypic splenic CD8^{–} or CD8^{+} DCs) are indicated. These results are representative of 3 independent experiments with similar results. **e**, IFN-α production by donor-type B220[+]-DCs. RT–PCR analysis of IFN-α mRNA expression by FACS-sorted Ly5.2[+] B220[+]-DCs after culture in the absence (a) or the presence (b) of Sendai virus.
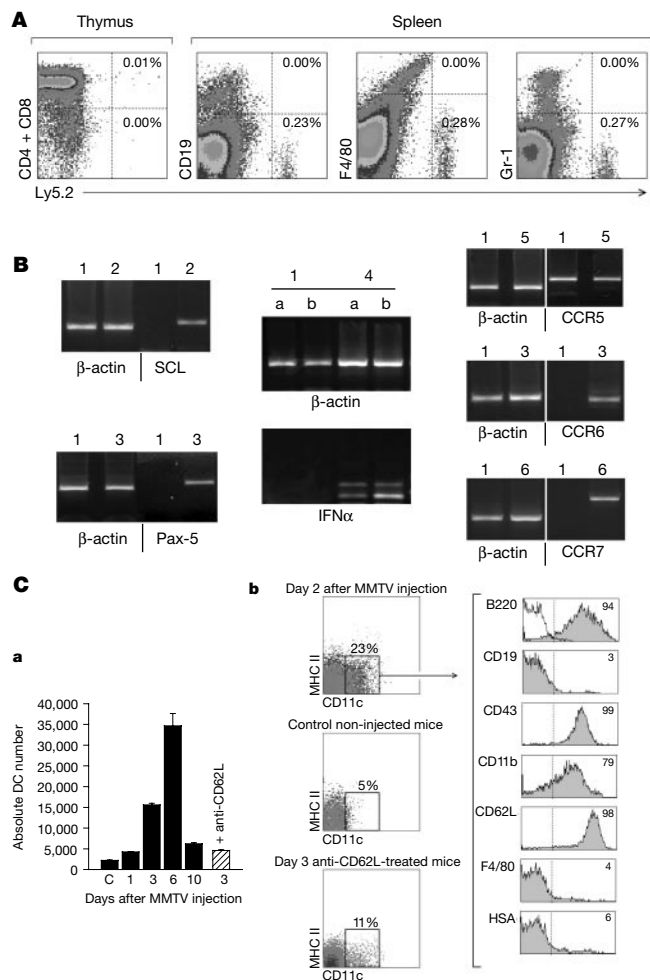
Figure 3 Links with myeloid and lymphoid lineages and homing potential of DC-precursors. **A**, Non-DC reconstitution potential of DC-precursors. Analysis performed on total thymus or spleen cell suspensions, 14 days after DC-precursor transfer into irradiated recipients, showing that no T cells, B cells, monocytes, macrophages, or granulocytes were generated from DC-precursors. (Note that the minute population of Ly5.2$^+$ CD8$^+$ thymic cells corresponds to CD8$^+$ DCs, as confirmed by our data on thymic DC reconstitution from DC-precursors, and that no monocytes or macrophages were found among DC-precursor progeny, since no donor-type Gr-1$^+$ and/or F4/80^{high} cells were found, Ly5.2$^+$ F4/80^{low} cells corresponding to reconstituted CD11c$^+$ splenic DCs. **B**, RT–PCR analysis of SCL, Pax-5, IFN-α, CCR5, CCR6 and CCR7 mRNA expression by DC precursors. 1 : DC-precursors; 2: bone marrow cells; 3: splenic B cells; 4: peritoneal macrophages; 5, CD8$^+$ DCs; 6, CD40-stimulated Langerhans cells; a, b: 18 hour-culture in the absence (a) or presence (b) of Sendai virus. **C**, DC-precursor recruitment during MMTV infection. **a**, Absolute lymph node DC number at the indicated time points after MMTV injection. Data represent the mean ± s.d. (n = 3). **b**, Characterization of CD11c$^+$ MHC-II$^-$ DC-precursors in the lymph node at day 2 after virus injection. These results are representative of three experiments with similar results.

day 2 after MMTV injection, and around 3.5×10^4 DCs were found at day 6, suggesting a 5-fold expansion. In order to further explore the mechanisms involved in the migration of DC-precursors, these were analysed for the expression of the chemokine receptors CCR5, CCR6 and CCR7 known to participate in DC homing and migration[1]. Neither CCR6- nor CCR7-mRNA was expressed by DC-precursors (Fig. 3B). However, DC-precursors expressed CCR5, which has been claimed to be involved in immature DC migration[18], and could therefore control DC-precursor homing to lymphoid organs. □

Methods

Blood DC-precursor isolation

DC-precursors were isolated from lysis-buffer-treated heparinized blood by depletion (at a 7:1 bead-to-cell ratio) with magnetic beads (Dynal) coated with anti-rat immunoglobulins (Igs) and mouse Igs, after incubation with monoclonal antibodies anti-CD3, CD4, CD8α, MHC-II, HSA, F4/80 and Gr-1 (purity >90%; Fig. 1A, b). Highly purified DC-precursor populations with a purity >98% were then obtained by magnetic cell sorting (MACS; Miltenyi Biotec) after incubation with anti-CD11c-conjugated microbeads (Fig. 1A, c), or fluorescence-activated sorting (FACS).

Reconstitution experiments with DC-precursors

5×10^5 DC-precursors purified from C57 BL/Ka Ly 5.2 donor mice were injected intravenously into γ-irradiated (7 Gy) C57 BL/6 Ly 5.1 Pep^{3b} recipient mice, along with 4×10^4 Ly 5.1 bone marrow cells to ensure survival of recipients. Donor-type DCs were analysed on B220$^-$ or B220$^+$ splenic DC-enriched fractions obtained from spleen low-density fractions, after magnetic bead depletion of cells expressing B220, CD3 or Gr-1 (B220$^-$ fraction) or expressing Igs, CD3 or Gr-1 (B220$^+$ fraction). Analysis of DC-precursor expansion was performed after labelling of purified DC-precursors with the intracellular fluorescent dye carboxyfluorescein diacetate succinimidyl ester (CFSE; Molecular Probes) at 1 μM for 10 min at 37 °C.

Flow cytometry

Analysis of blood DC-precursors and lymph node CD11c^{int} MHC-II$^-$ cells were performed after staining with fluorescein (FITC)-conjugated anti-CD11c, phycoerythrin (PE)-conjugated anti-MHC-II and biotin-conjugated anti-B220, CD19, CD43, CD11b, Thy-1, CD62L, FcRγII/III, CD44, c-kit, IL-7Rα, IL-3Rα, CD40, CD86, DEC-205, F4/80 or HSA, followed by streptavidin-TriColor (Caltag Laboratories). Analysis of CD8$^-$ and CD8$^+$ DC reconstitution was performed after staining with FITC-conjugated anti-Ly5.2, PE-conjugated anti-CD8α and biotin-conjugated anti-CD11c, followed by streptavidin-TriColor. Analysis of B220$^+$-DC reconstitution was performed after staining with FITC-conjugated anti-Ly5.2, PE-conjugated anti-B220 and biotin-conjugated anti-CD11c, followed by streptavidin-TriColor. Analysis of Ly5.2$^+$ DC phenotype was performed after staining with FITC-conjugated anti-Ly5.2, PE-conjugated anti-CD11c and biotin-conjugated anti-MHC II or DEC-205, followed by streptavidin-TriColor. Analysis of CD40 expression by Ly5.2$^+$ B220$^-$ or B220$^+$-DCs was performed after staining with FITC-conjugated anti-Ly5.2, PE-conjugated anti-B220 and biotin-conjugated anti-CD40 followed by streptavidin-TriColor. Analysis of CD40 expression by Ly5.2$^+$ CD8$^-$ or CD8$^+$ DCs was performed after staining with FITC-conjugated anti-Ly5.2, PE-conjugated anti-CD8α and biotin-conjugated anti-CD40 followed by streptavidin-TriColor. Analysis of CFSE profile of DC-precursors after transfer was performed after staining with PE-conjugated anti-CD11c and biotin-conjugated anti-Ly5.2 followed by streptavidin-TriColor.

Electron microscopy

FACS-sorted DC-precursors were fixed with 1% glutaraldehyde and 1% paraformaldehyde in 0.1 M pH 7.6 Sørensen phosphate buffer for 1 h at 4 °C, postfixed with 1% OsO4 in the same buffer for 1 h at 4 °C, dehydrated in graded acetone solutions, and embedded in Embed-812 (Electron Microscopy Sciences).

Detection of IFNα–mRNA

Purified DC-precursors, or FACS-sorted donor-type splenic B220$^+$-DCs isolated at day 10 after transfer of DC-precursors, were cultured for 18 h alone or in the presence of 10^6 p.f.u ml^{-1} Sendai virus (strain Z) and analysed for the expression of IFNα-mRNA by RT–PCR.

In vitro culture of DC-precursors

Generation of B cells and myeloid cells was assessed after culture of purified DC-precursors on S17 stromal cells at 10^5 cells ml^{-1} in 96-well plates, in the presence of 1 ng ml^{-1} murine IL-7, as described elsewhere[19]. Cultures were analysed at day 12 for the presence of myeloid cells and/or B cells on the basis of the expression of CD11c/Gr-1 and B220/CD19, respectively. NK cell generation was assessed after culture in the presence of 10^3 U ml^{-1} murine IL-2, as described elsewhere[20]. Cultures were analysed at day 5 for the presence of cells expressing the pan-NK cell marker DX5.

Analysis of DC-precursors during MMTV infection

BALB/c mice were given a 10 μl injection (10^9 virus particles) of MMTV (strain SW), in the hind footpad and the draining popliteal lymph nodes were analysed. Characterization of CD11c^{int} MHC-II$^-$ cells was performed after magnetic bead depletion of cells positive for Igs, CD3 or Gr-1, by gating on cells with low forward and side scatter. Blocking of DC-precursor migration to the lymph nodes via high endothelial venules was achieved by intravenous injection of purified anti-CD62L antibodies (clone Mel-14) into mice which were injected 24 h before with MMTV(SW), and subsequently analysed by day 3.

RT–PCR

mRNA was purified from FACS-sorted cells with magnetic beads (mRNA direct micro kit; Dynal), reverse transcribed and subjected to PCR amplification using the following primers: SCL (sense): 5′-GTT TTG GTC TAG AGT TTG TGA GCC-3′; SCL (anti-sense):

5′-GCA TGC TCA AGG CTG CTG ACT TGG-3′. Pax-5 (sense): 5′-CTACAGGCTCC GTGACGCAG-3′; Pax-5 (anti-sense): 5′-TCT CGG CCT GTG ACA ATA GG-3′. CCR5 (sense): 5′-ACT GGG GTG GTG GCT GTG TTT-3′; CCR5 (anti-sense): 5′-TTG TCT TGC TGG AAA ATT GAA-3′. CCR6 (sense): 5′-CTG CAG TTC GAA GTC ATC-3′; CCR6 (anti-sense): 5′-GTC ATC ACC ACC ATA ATG TTG-3′. CCR7 (sense): 5′-AGC ACC ATG GAC CCA GGG AAA CC-3′; CCR7 (anti-sense): 5′-CAG CAT CCA GAT GCC CAC A-3′. IFN-α (sense): 5′-TGT CTG ATG CAG CAG GTG G-3′; IFN-α (anti-sense): 5′-AAG ACA GGG CTC TCC AGA C-3′. PCR conditions were: SCL: 30 s/95 °C; 30 s/60 °C; 60 s/72 °C. Pax-5: 15 s/94 °C; 90 s/65 °C. CCR5: 15 s/94 °C; 30 s/57 °C; 60 s/72 °C. CCR6: 15 s/94 °C; 15 s/59 °C; 45 s/72 °C. CCR7: 15 s/94 °C; 90 s/68 °C. IFN-α: 40 s/94 °C; 40 s/62 °C; 60 s/ 72 °C. PCR products were: SCL: 425 bp; Pax-5: 439 bp; CCR5: 539 bp; CCR6: 320 bp; CCR7: 561 bp; IFN-α: 166 bp.

Langerhans cell stimulation

CD40-stimulated Langerhans cells, used as positive control for CCR7 expression, were isolated from the ear epidermis and cultured for 48 h with 100 µg ml⁻¹ anti-CD40 monoclonal antibody, as described elsewhere[21].

1. Bancherau, B. et al. Immunobiology of dendritic cells. Annu. Rev. Immunol. 18, 767–811 (2000).
2. Martín, P. et al. Concept of lymphoid versus myeloid dendritic cell lineages revisited: both CD8α⁻ and CD8α⁺ dendritic cells are generated from CD4^low lymphoid–committed precursors. Blood 96, 2511–2519 (2000).
3. Traver, D. et al. Development of CD8α-positive dendritic cells from a common myeloid progenitor. Science 290, 2152–2154 (2000).
4. Manz, M. G., Traver, D., Miyamoto, T., Weissman, I. L. & Akashi, K. Dendritic cell potentials of early lymphoid and myeloid progenitors. Blood 97, 3333–3341 (2001).
5. Anjuère, F. et al. Definition of dendritic cell subpopulations present in the spleen, Peyer's patches, lymph nodes and skin of the mouse. Blood 93, 590–598 (1999).
6. Martínez del Hoyo, G., Martín, P., Fernández Arias, C., Rodríguez-Marín, A. & Ardavín, C. CD8α⁺ dendritic cells originate from the CD8α⁻ dendritic cell subset by a maturation process involving CD8α, DEC-205 and CD24 upregulation. Blood 99, 999–1004 (2002).
7. Ardavín, C., Wu, L., Li, C. L. & Shortman, K. Thymic dendritic cells and T cells develop simultaneously in the thymus from a common precursor population. Nature 362, 761–763 (1993).
8. Martín, P. et al. Characterization of a new subpopulation of mouse CD8α⁺ B220⁺ dendritic cells with tolerogenic potential. Blood (submitted).
9. Akashi, K., Traver, D., Miyamoto, T. & Weissman, I. L. A clonogenic common myeloid progenitor that gives rise to all myeloid lineages. Nature 404, 193–197 (2000).
10. Mebius, R. E. et al. The fetal liver counterpart of adult common lymphoid progenitors gives rise to all lymphoid lineages, CD45⁺CD4⁺CD3⁻ cells, as well as macrophages. J. Immunol. 166, 6593–6601 (2001).
11. Kondo, M., Weissman, I. L. & Akashi, K. Identification of clonogenic common lymphoid progenitors in mouse bone marrow. Cell 91, 661–672 (1997).
12. Lyman, S. D. & Jacobsen, S. E. W. c-kit ligand and flt3 ligand: Stem/progenitor cell factors with overlapping yet distinct activities. Blood 91, 1101–1134 (1998).
13. Singh, H. Gene targeting reveals a hierarchy of transcription factors regulating specification of lymphoid cell fates. Curr. Opin. Immunol. 8, 160–165 (1996).
14. Mojica, M. P. et al. Phenotypic distinction and functional characterization of pro-B cells in adult mouse bone marrow. J. Immunol. 166, 3042–3051 (2001).
15. Siegal, F. P. et al. The nature of the principal type 1 interferon-producing cells in human blood. Science 284, 1835–1837 (1999).
16. Cella, M. et al. Plasmacytoid monocytes migrate to inflamed lymph nodes and produce large amounts of type I interferon. Nature Med. 5, 919–923 (1999).
17. Ardavín, C. et al. B cell response after MMTV infection: extrafollicular plasmablasts represent the main infected population and can transmit viral infection. J. Immunol. 162, 2538–2545 (1999).
18. Sozzani, S. et al. Cutting edge: Differential regulation of chemokine receptors during dendritic cell maturation: A model for their trafficking properties. J. Immunol. 161, 1083–1086 (1998).
19. Tudor, K.-S. R. S., Payne, K. J., Yamashita, Y. & Kincade, P. W. Functional assessment of precursors from murine bone marrow suggests a sequence of early B lineage differentiation events. Immunity 12, 335–345 (2000).
20. Rolink, A. et al. A subpopulation of B220⁺ cells in murine bone marrow does not express CD19 and contains natural killer cell progenitors. J. Exp. Med. 183, 187–194 (1996).
21. Anjuère, F., Martínez del Hoyo, G., Martín, P. & Ardavín, C. Langerhans cells acquire a CD8⁺ dendritic cell phenotype on maturation by CD40 ligation. J. Leukocyte Biol. 67, 206–209 (2000).

Competing interests statement

The authors declare that they have no competing financial interests.

Correspondence and requests for materials should be addressed to C.A. (e-mail: ardavin@bio.ucm.es).

A blue-light-activated adenylyl cyclase mediates photoavoidance in *Euglena gracilis*

Mineo Iseki*†‡, Shigeru Matsunaga§, Akio Murakami‖, Kaoru Ohno*, Kiyoshi Shiga¶, Kazuichi Yoshida*, Michizo Sugai#, Tetsuo Takahashi☆, Terumitsu Hori§ & Masakatsu Watanabe*††

* National Institute for Basic Biology, Okazaki, Aichi, 444-8585 Japan
† Bio-oriented Technology Research Advancement Institution, 3-18-19, Toranomon, Minato-ku, Tokyo, 105-0001 Japan
‡ Center for Gene Research, Nagoya University, Furo-cho, Chikusa-ku, Nagoya, 464-8602 Japan
§ Institute of Biological Sciences, University of Tsukuba, Tsukuba, Ibaraki, 305-8572 Japan
‖ Kobe University Research Center for Inland Seas, Iwaya, Awaji, Hyogo, 656-2401 Japan
¶ Department of Physiology, Kumamoto University School of Medicine, Honjo, Kumamoto, Kumamoto, 860-8556 Japan
# Department of Biology, Faculty of Science, Toyama University, Toyama, Toyama, 930-8555 Japan
☆ School of Pharmaceutical Sciences, Toho University, 2-2-1, Miyama, Funabashi, Chiba, 274-8510 Japan
†† Department of Photoscience, School of Advanced Sciences, Graduate University for Advanced Studies, Shonan Village, Hayama, Kanagawa, 240-0193 Japan

Blue light regulates processes such as the development of plants and fungi and the behaviour of microbes[1,2]. Two types of blue-light receptor flavoprotein have been identified: cryptochromes, which have partial similarity to photolyases[3,4], and phototropins, which are photoregulated protein kinases[5,6]. The former have also been found in animals with evidence of essential roles in circadian rhythms[7,8]. *Euglena gracilis*, a unicellular flagellate, abruptly changes its swimming direction after a sudden increase or decrease in incident blue light intensity, that is, step-up or step-down photophobic responses, resulting in photoavoidance or photoaccumulation, respectively[9]. Although these photobehaviours of *Euglena* have been studied for a century[10], the photoreceptor molecules mediating them have remained unknown[9]. Here we report the discovery and biochemical characterization of a new type of blue-light receptor flavoprotein, photoactivated adenylyl cyclase, in the photoreceptor organelle of *Euglena gracilis*, with molecular genetic evidence that it mediates the step-up photophobic response.

Action spectroscopy has indicated that one or more flavins are chromophores of the photoreceptor molecules for photophobic responses in *Euglena*[11,12]. The paraflagellar body (PFB), near the base of its flagellum and in the vicinity of the stigma, is considered as a photosensing organelle for photomovements[9] (see Fig. 4A). Its bright green autofluorescence supports the hypothesis that flavoproteins localized in the PFB might act as the photoreceptor molecule[13,14]. To examine this hypothesis we isolated PFBs and purified the flavoproteins from them.

The isolated PFBs (Fig. 1a) were solubilized by sonication in detergent and the flavoprotein was purified by anion-exchange chromatography, followed by gel filtration. The fraction of apparent molecular mass ~400,000 (M_r ~400K) showed the highest intensity of fluorescence at 530 nm after boiling to release noncovalently bound chromophores (see Fig. 3b), with excitation (peaking at 370 and 450 nm) and emission (peaking at 530 nm) spectra characteristic of flavins (Fig. 1b). The fluorescence excitation spectrum of the undenatured M_r 400K fraction also showed two peaks at 370 and 450 nm (Fig. 1b), consistent with the action spectra for photophobic responses of *Euglena*[12]. The fact that the fluorescence of the undenatured M_r 400K fraction was much weaker than

1047